



Letter to the Editors

Orientation of γ to α transformation in Xe-implanted austenitic 304 stainless steel

Guoqiang Xie¹, Minghui Song^{*}, Kazutaka Mitsuishi, Kazuo Furuya*National Research Institute for Metals, 3-13 Sakura, Tsukuba, Ibaraki 305-0003, Japan*

Received 3 April 2000; accepted 3 June 2000

Abstract

The phase transformation of γ (fcc) to α (bcc) is observed in thin film specimens of austenitic 304 stainless steel implanted with 100 keV ions at room temperature. The orientation relationships between the induced α (bcc) and the austenitic γ (fcc) matrix are determined to be $(01\bar{1})_{\alpha} // (1\bar{1}1)_{\gamma}$ and $[111]_{\alpha} // [011]_{\gamma}$. The relationship is followed by the Kurdjumov–Sachs (K–S) rule rather than the Nishiyama–Wasserman (N–W) rule in this experiment, though the latter relationship was well observed in the previously reported experiments of implantation of austenitic stainless steels with noble gases or other heavy ions. © 2000 Elsevier Science B.V. All rights reserved.

PACS: 64.70.–p; 81.30.Kf; 61.80.–x**1. Introduction**

The austenitic stainless steel is one of the most important materials in industry. It is also considered as the prospective candidate for the first wall materials of fusion reactors and the structural materials in the active zone of fast breeder reactors [1]. Researches have been carried out extensively for basic understanding of the behavior of the austenitic stainless steel in radioactive circumstances.

The first evidence for the occurrence of a martensitic phase transformation of γ (fcc) to α (bcc) in austenitic stainless steels after ion implantation was obtained with electron microscopy from 18/8 and 316 steels implanted with phosphorus [2,3]. Further researches with transmission electron microscopy (TEM), glancing angle X-ray diffraction (GXR), Rutherford backscattering (RBS), conversion electron Mössbauer spectroscopy (CEMS), revealed that im-

plantations with other energetic ions, such as Sb [4], inert gas ions (He, Ar, Kr and Xe) [5–9] and the constituent element ions (Fe, Ni and Cr) of the austenitic stainless steels [7,8], also induce the phase transformation. The orientation relationships of the transformed α -phase to the γ -matrix were observed and considered to agree with the Nishiyama–Wasserman (N–W) rule $(110)_{\alpha} // (111)_{\gamma}$ and $[1\bar{1}0]_{\alpha} // [\bar{2}11]_{\gamma}$ in the experiments of ion implantation of austenitic stainless steels, such as the experiments of P and Sb ions implantation of 18/8 and 316 stainless steels [2–4], and other experiments of ion implantation into austenitic stainless steels [8].

In our recent experiment, thin film specimens of 304 austenitic stainless steel (304SS) were implanted with 100 keV Xe ions to a fluence of 1.0×10^{21} ions m^{-2} at room temperature in a high-voltage transmission electron microscope (HVTEM). The orientation relationships between the induced α (bcc) phase and the austenitic γ (fcc) matrix were found to follow the Kurdjumov–Sachs (K–S) rule, namely, $(01\bar{1})_{\alpha} // (111)_{\gamma}$ and $[11\bar{1}]_{\alpha} // [10\bar{1}]_{\gamma}$ rather than the N–W rule, though it was reported to be the mostly observed relationship in ion implantation experiments of austenitic stainless steels. In this paper, we report and discuss the experimental results.

^{*} Corresponding author. Tel.: +81-298 59 5053; fax: +81-298 59 5054.

E-mail address: msong@nrim.go.jp (M. Song).

¹ Present address: Graduate School of Science and Technology, Niigata University, Niigata 950-2181, Japan.

2. Experimental

Thin foil disks, 3 mm in diameter and 0.2 mm in thickness, were cut out from the commercial grade 304SS foils, annealed at 1373 K for 0.5 h, then prepared into TEM specimens by electrolytical polishing using a twin jet technique in a solution of 90% acetic acid and 10% perchloric acid at 289 K. The Xe ion implantation was carried out at room temperature using ION/HVEM system which consists of 1000 keV HVTEM (JEM-ARM 1000), 200 and 30 keV ion implanters [10]. The accelerating voltage of Xe ions was 100 kV and the incident angle of the ion beam was 45°. The projected range and straggling of 100 keV Xe ions in 304SS calculated by TRIM code [11] were 17.9 and 6.2 nm, respectively. The electron beam was switched off during Xe ion implantation in order to eliminate the damages by electron irradiation. The specimens were implanted at a flux of 2.3×10^{17} ions $\text{m}^{-2} \text{s}^{-1}$. The largest fluence was 1.0×10^{21} ions m^{-2} . CTEM and HRTEM observations were performed at room temperature with the JEM-ARM 1000 TEM operated at 1000 kV during and after the Xe ion implantation.

3. Results and discussion

Defects were observed in the specimen implanted to a fluence larger than 2.0×10^{18} ions m^{-2} . The density of the defects increased with increasing the Xe ion fluence. After the specimen was implanted to a fluence of 4.3×10^{19} ions m^{-2} , extra spots were observed in selected area diffraction (SAD) patterns, suggesting that a phase transformation took place. Increasing the Xe ion implantation fluence, the fraction and the particle size of the induced phase increased. Fig. 1 shows the result of a specimen implanted to a fluence of 1.0×10^{20} ions m^{-2} . Figs. 1(a) and (b) give a bright field (BF) micrograph and the corresponding SAD pattern, respectively. New phase zones with sizes ranging from 10 to 30 nm are observed in Fig. 1(a) as shown by arrows. Extra spots are seen in the SAD pattern indicated by arrows in Fig. 1(b). Since the electron beam of the HVTEM was switched off during the Xe ion implantation, the morphology change and the new phase formation are considered as the results of the Xe ion implantation. As the fluence reached to 1.0×10^{21} ions m^{-2} , it was observed that almost all of the austenite $\gamma(\text{fcc})$ phase was transformed.

Fig. 2 presents a set of high-resolution transmission electron microscopy (HRTEM) micrographs and the corresponding SAD pattern of a specimen implanted to a fluence of 1.0×10^{20} ions m^{-2} . Fig. 2(a) shows a relatively large area in which the induced phase and the matrix are identified. The matrix of γ -phase in fcc structure is in $[0\ 1\ 1]$ direction. A part indicated by $\alpha(\text{bcc})$ is a crystal of bcc structure in $[1\ 1\ 1]$ direction. The lattice

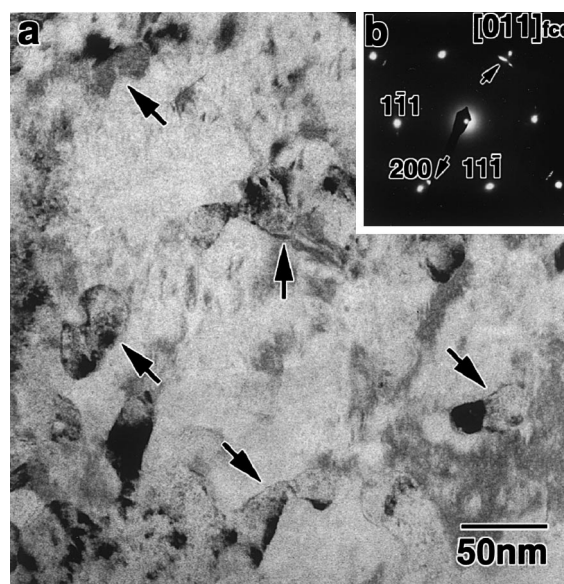


Fig. 1. Structure change of an austenitic 304 stainless steel specimen implanted with 100 keV Xe ions to a fluence of 1.0×10^{20} ions m^{-2} at room temperature: (a) a bright field (BF) TEM image; (b) the corresponding selected area diffraction (SAD) pattern.

planes of the bcc structure part are well consistent with the extra spots in the SAD pattern shown in Fig. 2(b), which confirms that the induced phase is in bcc structure. The induced bcc phase is considered as a martensite (α), since the lattice parameter obtained from both the diffraction pattern analysis and the HRTEM observation agrees with that of martensite, and that this kind of phase transformation was observed previously in ion implanted 304SS and other austenitic stainless steels [2–9]. Based on this consideration, the bcc part in Fig. 2(a) and the extra spots in the SAD pattern in Fig. 2(b) are indicated and suffixed to α . Figs. 2(c) and (d) show lattice images of the martensite bcc and the matrix fcc parts, respectively. Two figures were enlarged from the bcc and the matrix areas in Fig. 2(a) or the area close to Fig. 2(a) in the same TEM negative film. The lattice plane $(1\ \bar{1}\ 1)_\gamma$ in the matrix is oriented parallel to $(0\ 1\ \bar{1})_\alpha$ of the induced α -phase, as shown in the figures, so that the orientation relationships are obtained as $(0\ 1\ \bar{1})_\alpha // (1\ \bar{1}\ 1)_\gamma$ and $[1\ 1\ 1]_\alpha // [0\ 1\ 1]_\gamma$. These orientation relationships are confirmed to consist with the K–S rule, namely, $(0\ 1\ 1)_\alpha // (1\ 1\ 1)_\gamma$ and $[1\ 1\ \bar{1}]_\alpha // [1\ 0\ \bar{1}]_\gamma$, from the simulation of diffraction patterns. The K–S rule is one of the most commonly observed relationships of α/γ in conventional martensite transformation in steels but seldom observed in the previously reported ion implantation experiments. Only in a series of experiments of nitrogen-implanted 304 steels, the martensite was found to form in a ‘ γ to ϵ to α ’ transformation sequence

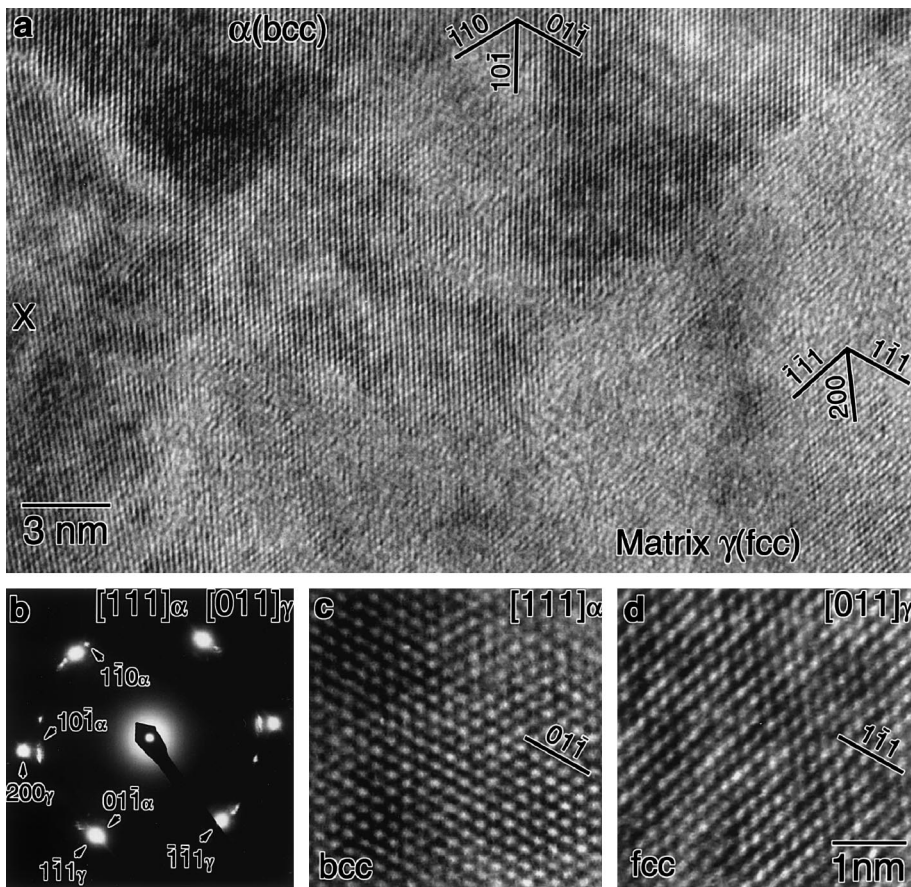


Fig. 2. HRTEM micrographs of an austenitic 304 stainless steel specimen implanted with 100 keV Xe ions to a fluence of 1.0×10^{20} ions m^{-2} at room temperature. (a) a relative large area; (b) the SAD pattern correspond to (a); (c) and (d) enlarged images of a bcc martensite area and a matrix area within or nearby (a).

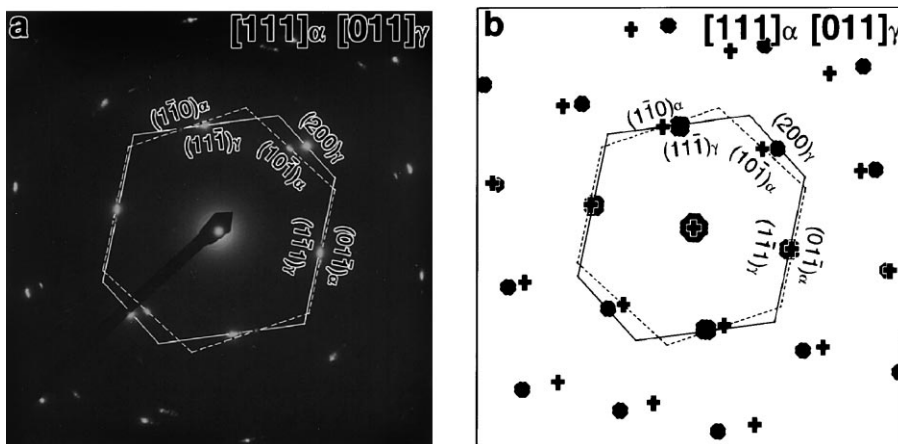


Fig. 3. An SAD pattern of an austenitic 304 stainless steel specimen implanted with 100 keV Xe ions to a fluence of 1.0×10^{20} ions m^{-2} at room temperature (a) and a simulated diffraction pattern (b) in $[1\ 1\ 1]_{\alpha} + [0\ 1\ 1]_{\gamma}$.

and the α/γ orientation relationship was found to follow the K–S rule [12]. It is probably that the ion implantation induced martensite transformation and orientation relationship of α/γ depend on the ion species or experimental conditions. There are also some areas observed with HRTEM which could not be explained as the matrix nor the bcc martensite structure. Such an area is indicated by X in Fig. 2(a). Further work should be carried out to clarify the nature of this area.

Fig. 3 gives an SAD pattern of a specimen in which the phase transformation was induced and the simulated diffraction pattern using the MacTempas program. Crystal face orientations corresponding to the diffraction spots of the matrix and the transformed α -phase in the SAD pattern are shown by the full-line and the broken-line, respectively. In Fig. 3(a), the matrix is in $[0\ 1\ 1]_\gamma$ and the α -phase is in $[1\ 1\ 1]_\alpha$ direction. The $(0\ 1\ \bar{1})_\alpha$ spot overlaps with the $(1\ \bar{1}\ 1)_\gamma$ spot in the Fig. 3(a), which means that the two lattice planes parallel to each other and have almost the same lattice spacing. Fig. 3(b) gives the simulated diffraction pattern corresponding to Fig. 3(a), namely, $[1\ 1\ 1]_\alpha + [0\ 1\ 1]_\gamma$, using the parameters of the two phases and the relationships of martensite to the matrix. The diffraction spots indicated by ‘dot’ sign are those of the fcc γ -phase, and those indicated by ‘plus’ sign are those of the bcc α -phase. The simulated results are well consistent with Fig. 3(a). This consistency confirms the orientation relationship between the α -phase and the γ -phase obtained in the previous paragraph.

4. Conclusion

The phase transformation of γ (fcc) to α (bcc) is observed in thin film specimens of austenitic 304 stainless steel implanted with 100 keV Xe ions at room temperature. The orientation relationships between the induced α (bcc) phase and the austenitic γ (fcc) matrix are determined to be $(0\ 1\ \bar{1})_\alpha // (1\ \bar{1}\ 1)_\gamma$ and $[1\ 1\ 1]_\alpha // [0\ 1\ 1]_\gamma$. The relationship is followed the Kurdjumov–Sachs (K–S) rule rather than the Nishiyama–Wassermann (N–W) rule in this experiment though the later relationship was well

observed in the previously reported experiments of implantation of austenitic stainless steels with noble gas ions or other heavy ions.

Acknowledgements

This work was supported by the Science and Technology Agency Japan under the center of excellence (COE) program entitled ‘the creation of advanced materials with atomic-scale structures exhibiting quantum phenomena’ at National Research Institute for Metals.

References

- [1] M.D. Donne, D.R. Baskes, G. Kalinen, R. Mattas, S. Mori, *J. Nucl. Mater.* 215 (1994) 69.
- [2] E. Johnson, T. Wohlenberg, W.A. Grant, P. Hansen, L.T. Chadderton, *J. Microscopy* 116 (1979) 77.
- [3] E. Johnson, T. Wohlenberg, W.A. Grant, *Phase Transitions* 1 (1979) 23.
- [4] E. Johnson, U. Littmark, A. Johansen, C. Christodoulides, *Philos. Mag. A* 45 (1982) 803.
- [5] N. Hayashi, T. Takahashi, *Appl. Phys. Lett.* 41 (11) (1982) 1100.
- [6] N. Hayashi, I. Sakamoto, T. Takahashi, *J. Nucl. Mater.* 128&129 (1984) 756.
- [7] N. Hayashi, E. Johnson, A. Johansen, L. Sarholt-Kristensen, I. Sakamoto, in: *Proceedings of the International Conference on Martensitic Transformations*, The Japan Institute of Metals, Nara, Japan, 1986, p. 539.
- [8] E. Johnson, A. Johansen, L. Sarholt-Kristensen, L. Gråbæk, N. Hayashi, I. Sakamoto, *Nucl. Instrum. and Meth. B* 19&20 (1987) 171.
- [9] I. Sakamoto, N. Hayashi, B. Furubayashi, H. Tanoue, *J. Appl. Phys.* 68 (9) (1990) 4508.
- [10] K. Furuya, M. Piao, N. Ishikawa, T. Saito, *Mater. Res. Soc. Symp. Proc.* 439 (1997) 331.
- [11] J.F. Ziegler, J.P. Biersack, U. Littmark, in: J.F. Ziegler (Ed.), *The Stopping and Range of Ions in Solids*, Pergamon, New York, 1985.
- [12] S. Fayeulle, in: *Ion Implantation 1988*, TransTech., Aedermannsdorf, 1988, p. 327.